Journal of Structural Engineering & Applied Mechanics (2023) 6(5):441-454
DOI 10.31462/jseam.2023.05441454

RESEARCH ARTICLE

Beam-column joint modeling effects on the seismic response of a non-ductile reinforced concrete building

Sadik Can Girgin[1*], Ibrahim Serkan Misir[1], Faruk Polat[2]

[1] Dokuz Eylul University, Department of Civil Engineering, Izmir, Türkiye
[2] Polat Engineering, Izmir, Türkiye

Article History

Received 02 July 2023
Accepted 10 December 2023

Keywords

Beam-column joints
Seismic performance
Existing buildings
Non-seismic details

Abstract

Seismic performance evaluation of existing reinforced concrete buildings requires numerical approaches that reflect the damage modes that may arise from deficiencies in beam-column joints. In this study, the seismic performance of an existing reinforced concrete building with four stories was investigated by applying elastic and deformable beam-column joint models. The deformable beam-column joint model was verified using an exterior non-ductile beam-column joint test. The model included a rotational spring located at the joint with two connected nodes in a zero-length with rigid elements in the vicinity of frame elements. Moment- rotation relationships represent the joint behavior, and they were defined based on shear stresses and strains. After effective modeling of beam-column joints, it was aimed to obtain the cyclic behavior of the building model using non-linear time history analysis. For this purpose, scaled earthquake records were applied to the three-dimensional numerical model, and the results were compared in terms of inter-storey drift ratios, column and beam chord rotations, and base shear. It was determined that the exterior beam-column joints reached their strength and deformation capacity, while the beam and columns remained below their section deformation limits according to the Turkish Earthquake Code.

1. Introduction

Non-ductile reinforced concrete (RC) buildings, which emerged especially due to inadequacies in practice, were heavily damaged or completely/partially collapsed in previous earthquakes and showed non-ductile seismic performance [1]. Damages caused by bond loss and insufficient beam-column joint strength might reduce the lateral force capacity of the structures and might sometimes be the main factor causing the collapse of the structure. In Türkiye, most existing RC buildings were designed with respect to the Turkish Earthquake Code (1975) [2], and minimum dimensions and reinforcing details of RC elements were stipulated for the shear capacity of beam-column joints. However, the applicability of the specified requirements regarding the details that were achieved in construction practice was not sufficiently ensured [3] until these details were included in the next generation Turkish Earthquake Code (1998) [4]. In addition, improper anchorage in beam longitudinal reinforcements and large spacing of 90-degree transverse reinforcement details are typical

* Corresponding author (sadik.girgin@deu.edu.tr)
eISSN 2630-5763 © 2023 Authors. Publishing services by golden light publishing®.
This is an open-access article under the CC BY-NC-ND license (http://creativecommons.org/licenses/by-nc-nd/4.0/).

applications encountered in construction practice in Mediterranean countries. Fig. 1 shows the damage due to the non-seismic detailing of the beam-column connections.

There has been a significant effort in the literature, both experimental and numerical research, to focus on the earthquake response of inadequately detailed joints. Higazy et al. [5] performed interior beam-column subassemblies with different configurations using a shake table. They concluded that an axial pressure of approximately 5% applied to the column improves the performance of the beam-column joint under cyclic loading. This performance decreases by almost 50% when a 5% axial load is applied as the tensile strength. Hakuto et al. [6] tested six specimens using variables such as beam reinforcement length into the joint, hook details, and presence of transverse rebars on interior and exterior beam-column joints constructed before the 1970s. They showed improvement in beam-column joint performance with anchored beam reinforcements compared with current practice. Misir and Kahraman [7] tested exterior beam-column joint specimens (Fig. 1b) [9], representing buildings constructed before 1975 with insufficient detailing, and proposed a new seismic strengthening technique based on anchoring prefabricated SIFCON blocks to the joint region. They concluded that in the first cycle of the S1 specimen test, the contribution of the rotations in the column and beam elements to the peak drift was 37% and 61%, respectively. The first shear damage of the joint was observed in the push direction of the 16th cycle at a drift level of 0.5% and in the tensile direction of the 19th cycle at 0.75% drift level. At the end of the experiment, the contribution of the joint deformation to the peak drift was determined to be 66% due to the joint damage increasing its effect with the peak drift ratio of 0.5% [7].

Youssef and Ghobarah [10] developed a numerical model that considers shear effects and bond-slip deformations using springs for concrete and reinforcing steel with four rigid elements. Pampanin et al. [11] suggested a model reflecting the shear mechanism of a joint with pinching and flexural deformations near the connections for structures designed for vertical loads. Favvata et al. [12] proposed a model for corner joints that considers basic characteristics such as initial stiffness, concrete compressive strength, and strength degradation effects. Lowes and Altoontash [13] considered a joint model to examine the behavior of joints under cyclic loading with shear and bond slip effects with 4 nodes and 12 degrees of freedom (Fig. 2a). Mitra and Lowes [14] developed the existing model of Lowes and Altoontash [13] using approximately thirty different parameters. Zhao et al. [15] improved the joint model proposed by Mitra and Lowes [14] by adding bottle-shaped concrete compression struts and diagonal concrete and rebar springs in the joint instead of shear panel elements. The model was verified with six interior beam-column joint tests, and cyclic comparisons with the test results were in good agreement. Bayhan et al. [16] examined the nonlinear modeling of reinforced concrete frames using the scissors joint model, in which the change in seismic demands and the level of damage were measured using dynamic analysis. Shear deformation and the slip of the reinforcement were simulated using flexible beam-column joint models in 4-storey reinforced concrete frame models and with a rigid joint model. The analysis results showed that the flexible model has almost two times a more seismic demand than the rigid model. De Risi et al. [17] improved the scissor model by eliminating the need for additional springs at the joint. The proposed model shown in Fig. 2b considers a rotational spring element for moment– rotation relationships derived from the shear capacity of the joint. Shayanfar et al. [18] proposed a numerical model for monotonic behavior of exterior joints, including axial diagonal springs in joint panels and rotational springs for beams and columns. The model was calibrated with a vast amount of experimental data, including the effect of beam bar anchorage types, the existence of column intermediate bars, the loading application to obtain the principal stress, and joint deformations. They concluded that the axial load is an effective factor in the parameters of joint behavior. Girgin [19] studied the effect of modeling assumptions for column-beam connections on the performance evaluation of non-ductile reinforced concrete buildings. Numerical model was constructed with nonlinear truss elements for column-beam connections and fiber-based elements for beams and columns. Two-dimensional four- and six-

storey reinforced concrete frames were analyzed by performing incremental dynamic analyses [19]. Sahutoglu and Tasligedik [20] studied an N-M interaction model for joints accounting for axial load level changes and verified the model with an actual structure damaged in the Christchurch Earthquake (2011). Tasligedik [21] proposed a simplified numerical model for beam-column joints under varying axial loads in the scope of the strength hierarchy assessment methodology.

Within the scope of this study, the experimental cyclic response of a full-scale beam-column joint test was numerically verified using 1) the elastic joint model (Model A) and 2) the deformable joint model (Model B). Then, the cyclic performance of an existing non-ductile reinforced concrete (RC) structure example was investigated by employing Model A and Model B joint models and performing a set of nonlinear time history analyses. Structural performance indicators such as relative story drift ratios, chord rotations of beam and column elements, base shear forces, and inelastic deformations were obtained and compared for both models.

2. Numerical investigation of a beam–column joint

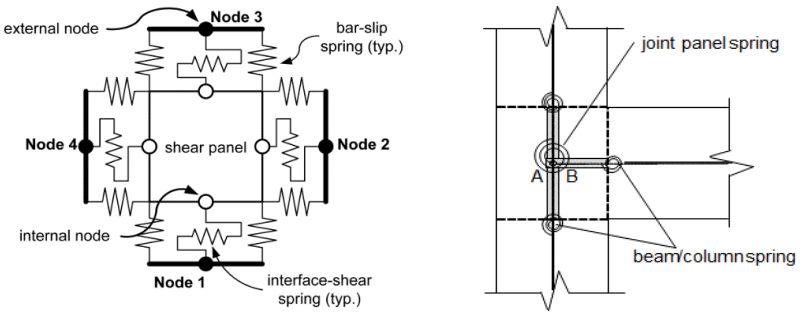
2.1. Beam-column joint test

Pantelides et al. [22] studied the cyclic behavior of exterior beam– column joints with non-seismic details depending on different beam longitudinal rebars and column axial load ratios (Fig. 3). A Unit-4 specimen with beam and column dimensions of 406 mm 406 mm was considered with an average concrete strength of 31.6 MPa and yield strengths of 469 MPa and 458.5 MPa for 25- and 29-mm diameter reinforcements, respectively. In the experiment, initial yielding in longitudinal reinforcement and clear cracks in the joint were observed at drift ratios of 0.5% and 1.5%, respectively. Shear damage and spalling of concrete occurred on the joint panel at 5% drift ratio.



(a) (b)

Fig. 1. Beam-column joint damages in (a) a residential building during 1999 Kocaeli Earthquake [8], and (b) a non-seismically detailed beam-column joint specimen [9]



(a) (b)

Fig. 2. (a) Beam-column joint macromodel by Lowes and Alttontash [13] and (b) beam-column joint model by De Risi et al. [17]

2.2. Beam-column joint model

A deformable joint model represented by a zero-length rotation spring is defined at the center of the joint panel. Two nodes are assigned to this spring, i.e., A and B, the column elements are attached to rigid links connected to node A, and the beam elements are attached to other rigid links connected to node B (Fig. 4) [23,24]. Beam and columns were considered with two integration points and force-based beam– column element formulation in OpenSees [25].

The four characteristic points of a multi-linear shear stress– strain relationship corresponding to cracking ($\gamma_{cr} = \%0.04, \tau_{cr}$), pre-peak ($\gamma = \%0.17;\ 0.85\tau_{max}$), peak, ($\gamma_{max} = \%0.49, \tau_{max}$) and residual deformation capacity ($\gamma_{res} = \%4.41;\ 0.43\tau_{max}$) limit states were obtained depending on the shear capacity of the corner joints, as in (Fig. 4). The shear deformation limits for the interior beam-column joints are assumed as $\gamma_{cr} = \%0.07$, $\gamma_{0.85} = \%0.6$, $\gamma_{max} = \%2.0$ and $\gamma_{res} = \%6.5$ [17].

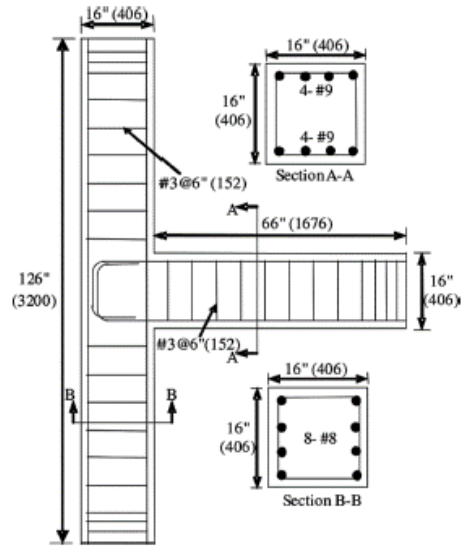
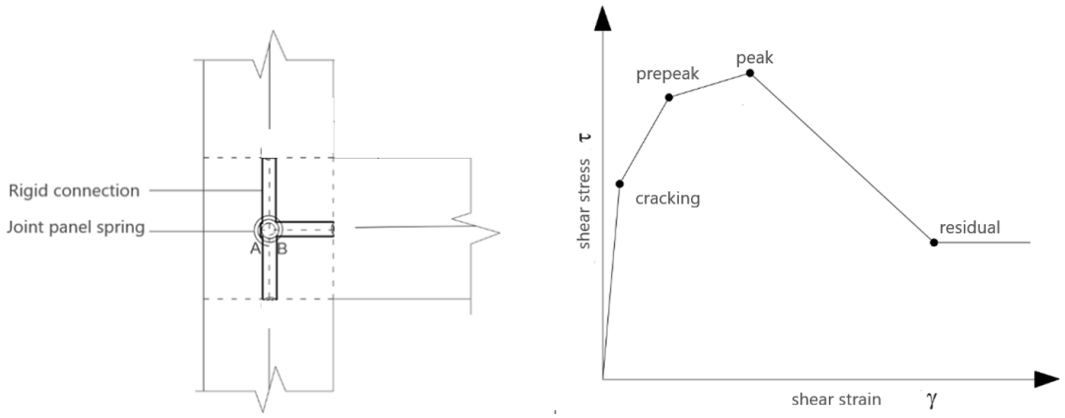


Fig. 3. Geometric and reinforcing details of the exterior Unit-4 specimen [26]



(a) (b)

Fig. 4. a) Deformable joint model for the exterior joint and b) shear stress– shear strain curves for the beam-column joint panel [23]

In the building model with deformable joints, moment– rotation relationships for cross-sections were defined for the joint panel spring, where M_j is the moment in the beam– column joint, A_j is the horizontal area of the panel, h_c is the cross-section dimension of the column in the relevant direction, L_b is the beam span, L_c is the column length in Eq. (1):

$$M_j = \tau_j \cdot A_j \frac{1}{\frac{1-\frac{h_c}{2L_b}}{jd_b} - \frac{1}{2L_C}} \tag{1}$$

The shear stress with the onset of the crack is obtained from Eq. (2), where P is the column axial load and fc is the concrete compressive strength.

$$\tau_{j,cr} = 0.29\sqrt{f_C}\sqrt{1 + 0.29\frac{P}{A_j}} \tag{2}$$

The maximum shear stress is given by Eq. (3) using the approach of Jeon et al. (2015)

$$\tau_{max} = 0.586(TB)^{0.774}(BI)^{0.495}(JP)^{1.25}(f_C)^{0.941} \tag{3}$$

where TB is the out-of-plane factor (in case of two beam connections, it is taken as 1.2), BI is the beam reinforcement index, and JP is the geometric factor (1.0 for interior joints, 0,75 for exterior joints). The moment-sectional rotation relations obtained depending on the shear capacities of the corner and interior beam-column joints were defined using the Pinching4 material model (Fig. 5) in OpenSees [25].

The concrete material model by Mander et al. [26] was used to calculate the stress– strain relationships in column and beam sections using the Concrete04 material model in OpenSees (Fig. 6a). The compressive strengths of the concrete core (fcc) for the beam and column were calculated as 35.2 MPa, while the corresponding strains (εcc ;εccu) were calculated as 0.0031 and 0.0065, respectively. For the reinforcing bars, the reinforcing steel model (Steel02) given in Fig. 6b was used with parameters R0 = 20, cR1 = 0.925, cR2 = 0.15 and Bs=0.02 [28].

2.3. Analysis results

The numerical cyclic response of the Unit-4 specimen was investigated using elastic joint (Model A) and deformable joint (Model B) modeling approaches. The deformable joint parameters were calculated and summarized in Table 1 along with joint shear stresses and corresponding moments and rotations. For Model A, the initial portion of the beam-column joint model up to the crack was defined, as shown in Fig. 4b. The load– displacement results obtained using the numerical models, where loading was applied from the cyclic beam end, are depicted in Fig. 7. Model A with the elastic joint approach (Fig. 7a) computed a value 1.5 times the horizontal load of the experimental study in the initial cycles. However, the deformable joint model (Model B) appropriately represented the cyclic behavior and stiffness and strength degradation with pinching of the beam-column joint specimen.

3. Existing reinforced concrete building example

The four-storey frame-type residential building example has the floor plan shown in Fig. 8 and 11 m 22 m plan dimensions [29]. The building has a story height of 3.85 m on the ground floor and 2.85 m on the other floors, resulting in a building height of 12.4 m. The structure was built on a ZD site class in an area with a high earthquake level ($0.75 \leq S_{DS}$). The characteristic values of the horizontal elastic acceleration spectrum are determined as $S_S = 1.15$, $S_1 = 0.288$, $F_S = 1.039$, $F_1 = 2.024$, $S_{DS} = 1.198$, and $S_{D1} = 0.583$, based on the current Turkish Earthquake Hazard Map (TEHM, 2021) by taking the ground motion level as DD2.

The highest ground acceleration is PGA=0.469 and the highest ground velocity is PGV=29.075, which is taken from the same digital map. The existing structure has beams with 25x50 cm and 30x50 cm cross-sections and columns with 25/50 cm, 30/70 cm, 25/60 cm, 30/60 cm, and 35/80 cm cross-sections with a slab thickness of 12 cm. The slab loads are transferred to each beam as a uniformly distributed load. Floor weights for the ground, upper, and top stories are 3116, 2748, and 1831 kN, respectively.

The three-dimensional models were constructed using STKO software (Scientific Toolkit for OpenSees) [30], as shown in Fig. 9, with different joint model assumptions. The average concrete compressive strength was 15 MPa. Core concrete parameters for each column were calculated. For the corner column, the corresponding stress (f_{cc}) and strains ε_{cc} and ε_{ccu} were calculated as 20.6 MPa, 0.0058, and 0.0118, respectively.

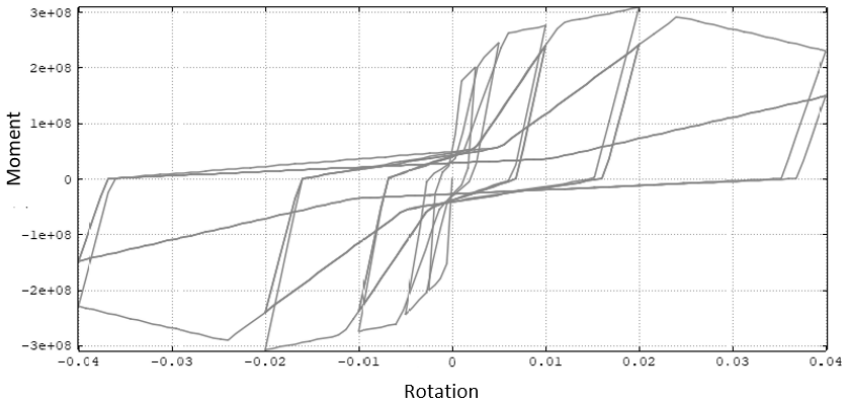
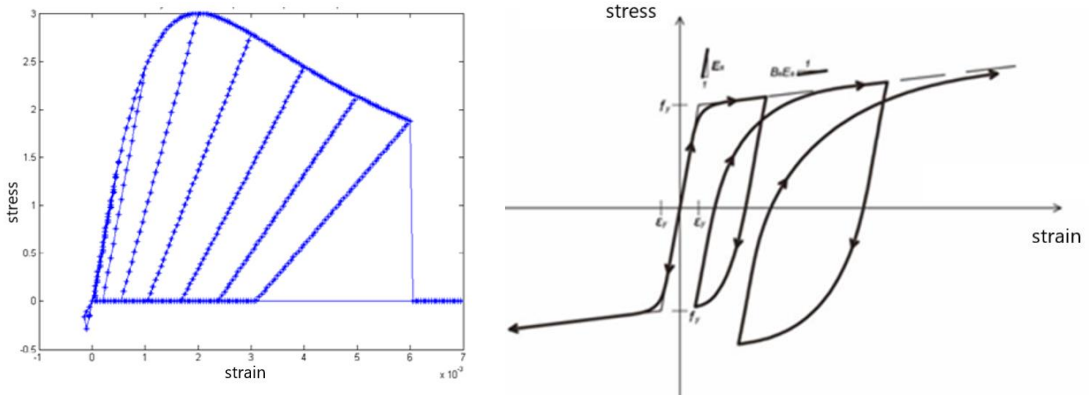


Fig. 5. Moment– rotation relationships for an interior beam–column joint

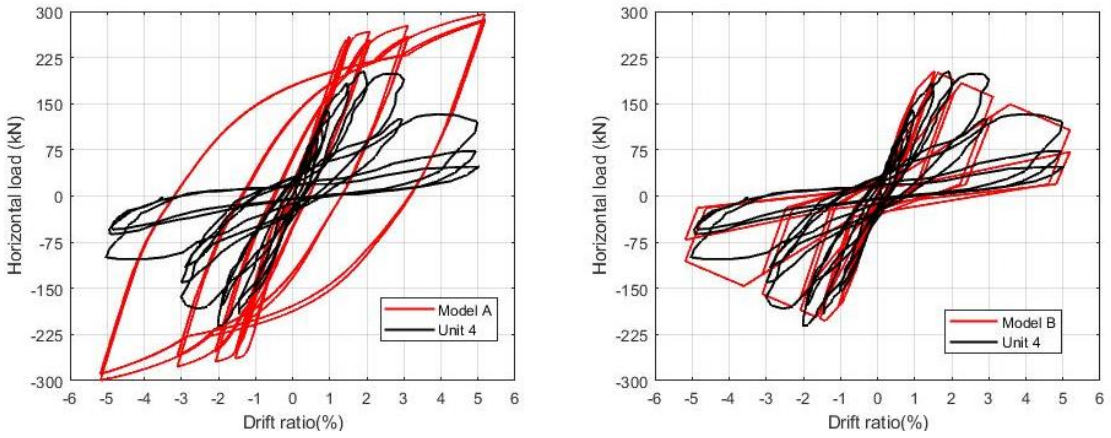


(a) (b)

Fig. 6. Hysteretic behavior of a) Concrete04 material model and b) Steel02 reinforcing steel material model

Table 1. Deformable joint model parameters for rotational springs in Unit-4 specimen

Stage	Shear stress (τ) (MPa)	Moment (M_j) (kNm)	Shear deformation (γ) (%)
Cracking	3.04	193.5	0.04
Pre-peak	4.54	289.0	0.17
Peak	5.34	340.0	0.49
Residual	2.29	146.2	4.41



(a) (b)

Fig. 7. Comparison of numerical and experimental behavior of Unit-4 specimen with (a) elastic joint model (Model A) and (b) deformable joint model (Model B)

The details of the deformable joint model used to simulate beam-column joints in an existing RC building are presented in Chapter 2. Deformable joint model parameters were obtained for the x and y directions for the interior, exterior, and corner beam-column joints of the existing structure. In this study, STKO was used as the OpenSees graphical user interface, which has been rapidly developed since the 2019 beta version. Each column and beam of the reference building were simulated by a frame element with five integration points using a force-based distributed plasticity behavior model. The first natural vibration period of the structure is calculated as $T_1 = 0.73\,s$.

4. Nonlinear time history analyses

4.1. Strong ground motion records

Scaled acceleration records used in the dynamic analyses were obtained in accordance with the Turkish Building Earthquake Code (TBEC) [31]. Horizontal design acceleration response spectra were obtained using the Türkiye Earthquake Hazard Map [32] for the existing structure, which was built on soil with local soil class ZD. Scaled acceleration was obtained by scaling 6 acceleration time histories from 4 different strong ground motions in the PEER database [33], as shown in Table 2, using SeismoMatch software [34]. As stated in TBEC (2018) [31], the averages of the scaled earthquake ground motion spectra shall not be less than the design spectrum ordinates for all periods. The suitability of the geometric mean of the spectrum curves obtained from the selected recordings to the target spectrum was compared with the largest and average mismatch values and was found to be appropriate. The converted records are also shown by superimposing the design spectrum (Fig. 10a). The spectrum averages obtained from the earthquake ground motion are shown in Fig. 10b.

4.2. Analysis results

The numerical model of the existing four-storey reinforced concrete building made of reinforced concrete frames is shown in Fig. 9a. KZ03 and KZ21 beams are supported to the SZ01 column at the corner joint on the ground floor of the building (Fig. 9b). Fig. 11 depicts the shear deformations in the beam– column joint (Fig.11.a) as well as the beam and column chord rotations for Model A with the elastic joint model and Model B with the deformable joint model (Figs.11.c and d) under the scaled Landers (1992) earthquake record as an example. The shear deformations given as γ_{23} and γ_{12} (Gama23 and Gama12) in the corner

beam-column joint are in the x and y directions, respectively. The exterior joint reaches shear deformation at the crack (0.04%) with 0.38% beam rotation and 0.58% column chord rotation, as shown in Fig. 11. The base shear-top displacement responses under the scaled Landers record show that (Fig. 12) the base shear capacity is reduced by 14% and 44% in the x and y directions, respectively, in Model B compared with Model A.

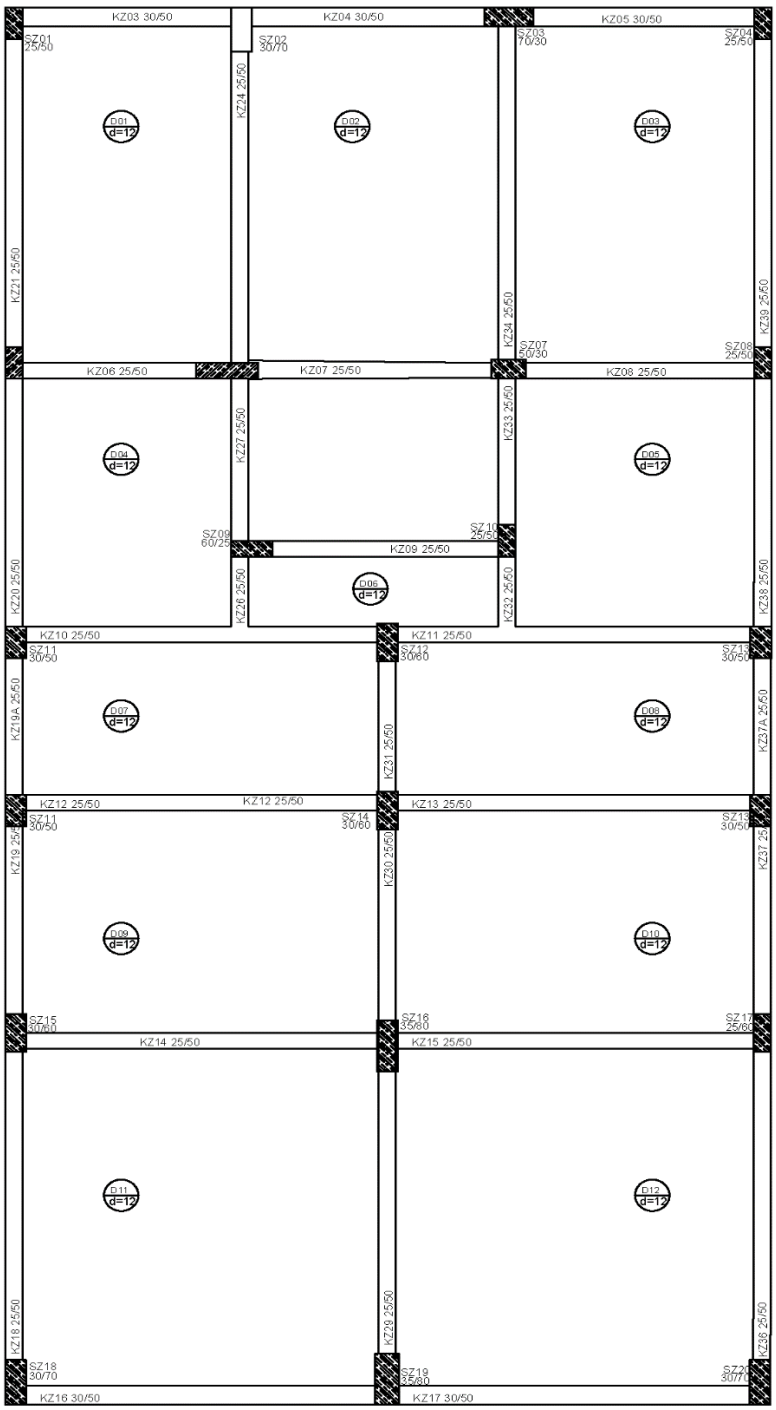
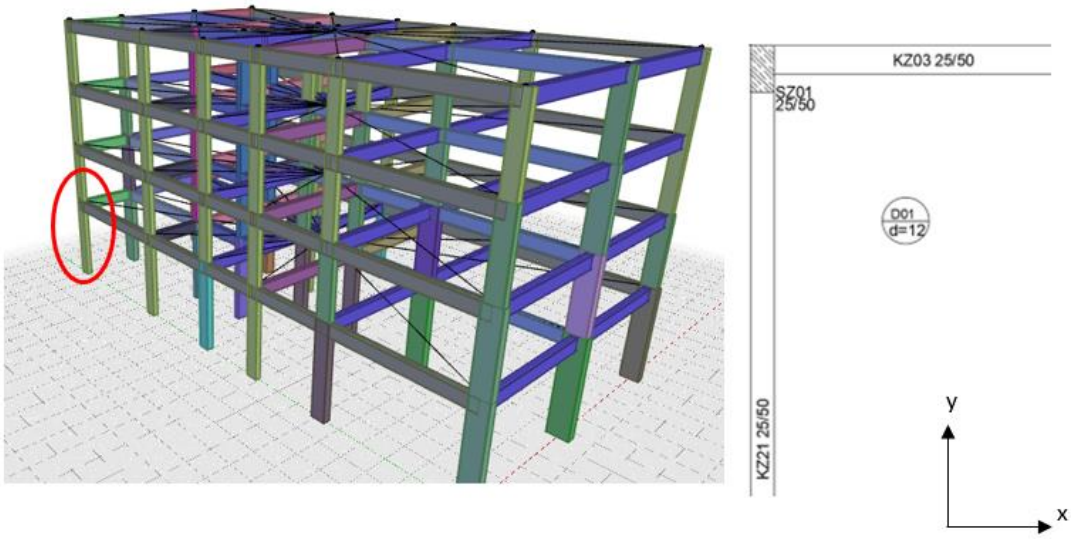
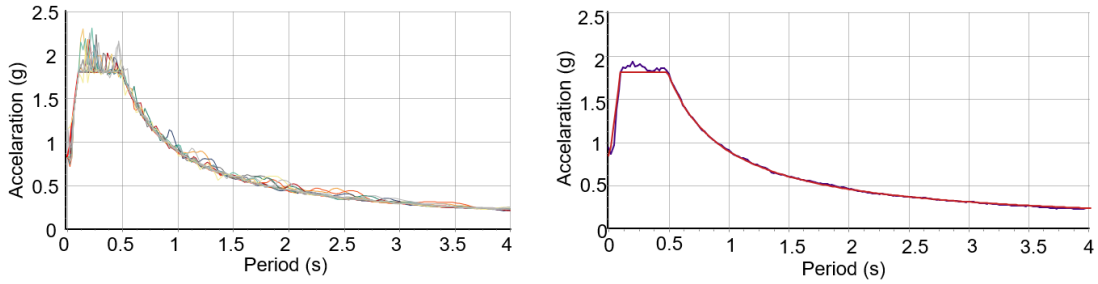


Fig. 8. Structural plan of the existing reinforced concrete building [29]



(a) (b)

Fig. 9. a) Numerical simulation model of the existing RC building and b) investigated corner beam-column joint [29]



(a) (b)

Fig. 10. a) Spectra of scaled strong ground acceleration records and b) average curve

Table 2. Selected and scaled strong ground motion records

No	Ground motion records	Mag	Year	H1 Rec	H2 Rec	Station
E1	Imperial Valley-06	6.53	1979	H-E12140	H-E12230	El Centro Array #12
E2	Superstition Hills-02	6.54	1987	B-WSM090	B-WSM180	Westmorland Fire Station
E3	Northridge-01	6.69	1994	FAI095	FAI185	El Monte- Fairview Avenue
E4	Landers	7.28	1992	ABY000	ABY090	Amboy
E5	Northridge-01	6.69	1994	PIC090	PIC180	LA- Pico and Sentous
E6	Landers	7.28	1992	BAK050	BAK140	Baker Fire Station

Joint shear deformations, corresponding drift ratios, and beam and column chord rotations were obtained and summarized for the six earthquake records, as shown in Fig. 13. The inter-storey drift ratios calculated for each story are shown in Figs. 13a and Fig. 13b. The joint deformations in the x and y directions for the achieved maximum story drift ratios under six earthquake records are presented in Figs. 13c and Fig. 13d for

Model B. It can be seen in the figures that the cracking strength of the joint ($\gamma_{cr} = 0.04\%$) reached a drift ratio of 0.32% in the x direction and 0.18% in the y direction on average. The deformation corresponding to the joint strength ($\gamma_{max} = 0.49\%$) reached a drift ratio of 1.48% in the x direction. In the y direction, it was determined that it reached an average drift ratio of 0.6%. It can be seen that the joint shear strength is reached before reaching the 1% drift ratio in both directions.

In addition, displaced axis rotations were calculated depending on the relative story drift ratio in columns and beams. When the peak deformation ($\gamma_{max} = 0.49\%$) corresponding to the shear strength of the joint was reached, the average section rotation in beam KZ03 in the x direction was calculated as 0.7%, and the largest section rotation in beam KZ21 in the y direction was calculated as 0.53% (Fig. 13e-f). Moreover, when the joint reached its shear strength, the average cross-sectional rotation in the x and y directions ($\theta_{y\text{-}y}$ and $\theta_{x\text{-}x}$) for the SZ01 column was calculated as 0.93% and 1.98%, respectively (Fig. 13g-h).

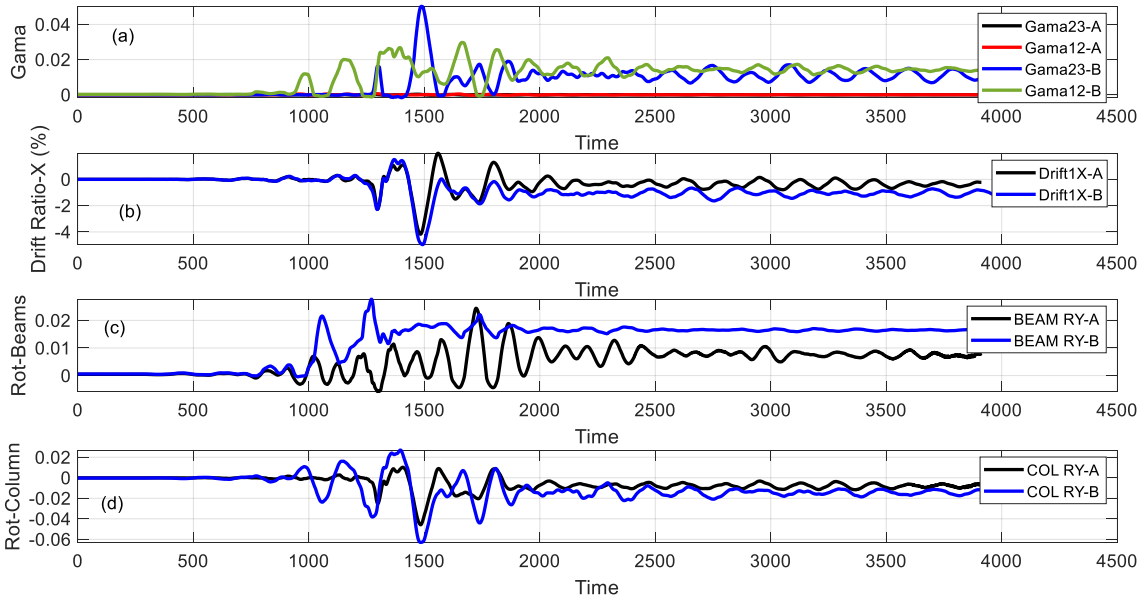
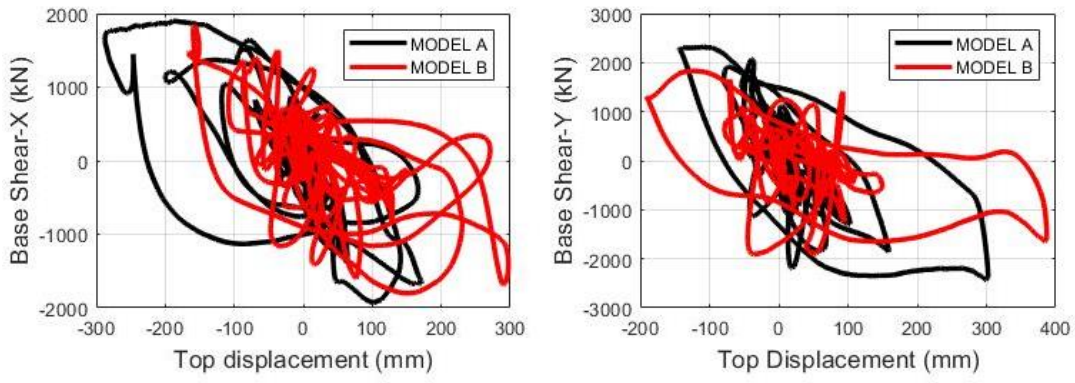


Fig. 11. (a) Shear deformations in the joint, (b) first-story drift ratio, and chord rotations of (c) beam and (d) column elements for the exterior joint considered.



(a) (b)

Fig. 12. Base shear-top displacement responses for buildings with Model A and B structural models in the (a) x direction and (b) y direction

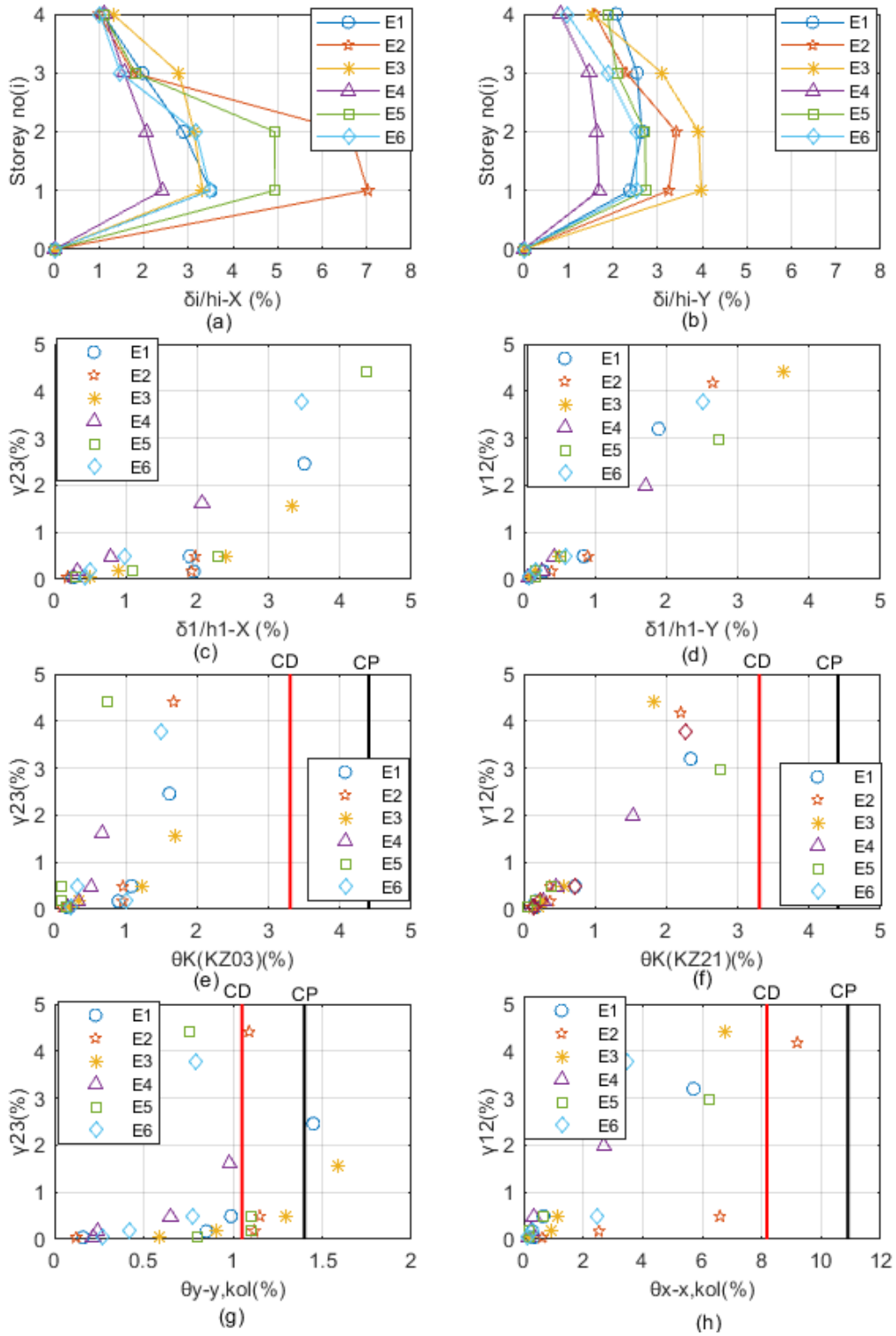


Fig. 13. (a-b) Drift ratio–building height, (c-d) joint shear deformation–drift ratio, (e-f) joint shear deformation–beam chord rotations, (g-h) joint shear deformation–column chord rotations

In TBEC (2018) [31], section deformation limits for controlled damage (CD) and collapse prevention (CP) damage states are defined in terms of plastic rotations and strains using the following equations :

$$\theta_P^{(CP)} = \frac{2}{3}\left[\left(\phi_u - \phi_y\right) L_P \left(1 - 0.5\frac{L_P}{L_S}\right) + 4.5\,\phi_u\, d_b\right] \quad (4)$$

$$\theta_P^{(CD)} = 0.75\,\theta_P^{(CP)} \quad (5)$$

where ϕ_u is ultimate curvature, ϕ_y is yield curvature, L_p is the plastic hinge length (0.5h), L_s is the shear span, and d_b is the beam bar diameter.

Accordingly, using XTRACT [35] software, the cross-sectional total rotation limits of the column at the collapse prevention (CP) limit state were calculated as 0.015 rad and 0.109 rad in the x and y directions, respectively. For beams, these values were 0.044 rad for the KZ03 beam and 0.047 rad for the KZ21 beam. As seen in Fig. 13 (g-h), the maximum shear strain ($\gamma_{max} = 0.49\%$) and the corresponding strengths of the joints are exceeded before reaching 1% chord rotation in the beams. Although we observed that the controlled damage (CD) performance limit was reached at the column in the short direction, it was determined that the maximum joint deformations ($\gamma_{max} = 0.49\%$) occurred earlier during the analyses.

5. Conclusion

In this study, the nonlinear behavior of an existing reinforced concrete frame-type building with insufficiently detailed beam-column joints was investigated by performing time history analyses. The interior, exterior, and corner beam-column joints of the building were represented by moment-rotation springs based on joint shear strength and deformation capacities. During the numerical analyses, the exterior beam– column joint and the beam and column element deformations were monitored. It was determined that the exterior beam–column joints had reached their cracking and residual deformations while the beam and column rotations were still below the section deformation limits given in the Turkish Building Earthquake Code (TBEC, 2018) [31]. The damage levels of reinforced concrete buildings may remain at a lower level with the assumption of rigid beam-column joints than those analyzed with the assumption of deformable beam-column joints for the performance assessment of a building with non-ductile joint details and a the lack of shear reinforcement. Neglecting joint deformations may lead to an overestimation of response for an existing building, as well as detailing the strengthening options for that structure. In addition, for existing reinforced concrete buildings with poorly detailed beam–column joints, it becomes necessary to limit the relative story drift ratios or to reduce the column and beam performance limits in determining seismic performance. Further numerical studies should be conducted by considering material models with bar slip, buckling, and rupture of reinforcement as well as axial load change in the beam-column joints.

Conflict of interests

The author(s) declared no potential conflicts of interest with respect to the research, authorship, and/or publication of this article.

Funding

This research received no external funding.

Data availability statement

No new data were created or analyzed in this study.

References

[1] Atmaca B, Arslan ME, Emiroğlu M, Altunışık AC, Adanur S, Demir A, Günaydın M, Kırtel O, Tatar T, BKahya V, Sunca F, Okur FY, Hacıefendioğlu K, Dok G, Öztürk H, Vural İ, Güleş O, Genç AF, Demirkaya E, Yurdakul M, Nas M, Akbulut YE, Baltacı A, Temel BA, Başağa HB, Sarıbıyık A, Şen F, Aykanat B, Öztürk İŞ, Navdar MB, Aydın F, Öntürk K, Utkucu M, Akgül T (2023) On the earthquake-related damages of civil engineering structures within the areas impacted by Kahramanmaraş earthquakes. Journal of Structural Engineering & Applied Mechanics, 6(2):98-116.

[2] Turkish Earthquake Code (1975) Regulation on Structures to be Built in Disaster Areas. Ankara, Türkiye.

[3] Aydinoglu MN (2007) From seismic coefficient to performance-based design: 40 years of earthquake engineering from an engineer's viewpoint. In: Proceedings of Sixth National Conference on Earthquake Engineering. Istanbul, Türkiye (In Turkish).

[4] Turkish Earthquake Code (1998) Regulation on Structures to be Built in Disaster Areas. Ankara, Türkiye.

[5] Higazy EMM, Elnashai AS, Agbabian MS (1996) Behavior of beam-column connections under axial column tension. Journal of Structural Engineering 122(5):501-511.

[6] Hakuto S, Park R, Tanaka H (2000) Seismic load tests on interior and exterior beam-column joints with substandard reinforcing details. Structural Journal 97(1):11-25.

[7] Misir IS, Kahraman S (2013) Strengthening of non-seismically detailed reinforced concrete beam–column joints using SIFCON blocks. Sadhana 38(1):69-88.

[8] Sezen H (1999) Damage to beam-column joint. Available at: http://nisee.berkeley.edu/elibrary.

[9] Misir IS (2011) Use of Slurry Infiltrated Fiber Concrete (SIFCON) in Improving the Seismic Behavior of Reinforced Concrete Structures. PhD Thesis, Dokuz Eylül University (in Turkish).

[10] Youssef M, Ghobarah A (2001) Modelling of RC beam-column joints and structural walls. Journal of earthquake engineering 5(01):93-111.

[11] Pampanin S, Magenes G, Carr A (2003) Modelling of shear hinge mechanism in poorly detailed RC beam-column joints. Proc. FIB Symp. Concrete Structures in Seismic Regions, Federation International du Beton, Athens. Paper No. 171.

[12] Favvata MJ, Izzuddin BA, Karayannis CG (2008) Modelling exterior beam–column joints for seismic analysis of RC frame structures. Earthquake Engineering & Structural Dynamics 37(13):1527-1548.

[13] Lowes LN, Altoontash A (2003) Modeling reinforced-concrete beam-column joints subjected to cyclic loading. Journal of Structural Engineering 129(12):1686-1697.

[14] Mitra N, Lowes LN (2007) Evaluation, calibration, and verification of a reinforced concrete beam–column joint model. Journal of Structural Engineering 133(1):105-120.

[15] Zhao W, Yang H, Chen J, Sun P (2019) A proposed model for nonlinear analysis of RC beam-column joints under seismic loading. Engineering Structures 180:829-843.

[16] Bayhan B, Özdemir G, Gülkan P (2017) Impact of joint modeling approach on performance estimates of older-type RC buildings. Earthquake Spectra 33(3):1101-1123.

[17] De Risi MT, Ricci P, Verderame GM (2017) Modelling exterior unreinforced beam-column joints in seismic analysis of non-ductile RC frames. Earthquake Engineering & Structural Dynamics 46(6):899-923.

[18] Shayanfar J, Hemmati A., Bengar HA (2019) A simplified numerical model to simulate RC beam–column joints collapse. Bulletin of Earthquake Engineering 17(2):803-844.

[19] Girgin SC (2020) Effect of Modeling beam-column joints on performance assessment of columns in non-ductile RC frames. Teknik Dergi 31(6):10339-10358.

[20] Sahutoglu O, Tasligedik AS (2021) Numerical case studies towards the validation of an RC beam-column joint N-M interaction model. In: Proceedings of 6ICEES: 6th International Conference on Earthquake Engineering and Seismology. Kocaeli, Turkey.

[21] Tasligedik A. (2023) State-of-art summary of the strength hierarchy assessment and its applications. Journal of Structural Engineering & Applied Mechanics 6(1):1-9.

[22] Pantelides CP, Hansen J, Nadauld J, Reaveley LD (2002) Assessment of reinforced concrete building exterior joints with substandard details. PEER Report 2002/18.

[23] Jeon JS, Lowes LN, DesRoches R, Brilakis I (2015) Fragility curves for non-ductile reinforced concrete frames that exhibit different component response mechanisms. Engineering Structures 85:127-143.

[24] Ricci P, Manfredi V, Noto F, Terrenzi M, de Risi MT, Di Domenico M, Camata G, Franchin P, Masi A, Mollaioli F, Spacone E, Verderame GM (2019) RINTC-E Towards seismic risk assessment of existing residential reinforced concrete buildings in Italy. In: Proceedings of COMPDYN 2019: 7th ECCOMAS Thematic Conference on Computational Methods in Structural Dynamics and Earthquake Engineering, Crete, Greece.

[25] McKenna F, Fenves GL, Scott MH, Jeremic B (2000) Open System for Earthquake Engineering Simulation (OpenSees).

[26] Sharma A, Eligehausen R, Reddy GR (2013) Pivot hysteresis model parameters for reinforced concrete columns, joints and structures. ACI Structural Journal 110(2):217-227.

[27] Mander JB, Priestley MJ, Park R (1988) Theoretical stress-strain model for confined concrete. Journal of Structural Engineering 114(8):1804-1826.

[28] Filippou FC, Popov EP, Bertero VV (1983) Effects of bond deterioration on hysteretic behavior of reinforced concrete joint. Earthquake Engineering Research Center. Report No: UCB/EERC-83/19.

[29] Polat F (2021) Investigation of strain-based performance limits in reinforced concrete buildings with inadequately detailed beam-column joints, MSc Thesis, Dokuz Eylul University.

[30] Petracca M, Candeloro F, Camata G (2017) STKO User Manual. ASDEA Software Technology, Pescara, Italy.

[31] Turkish Earthquake Building Code TBEC (2018) Disaster and Emergency Management Presidency. Ankara, Türkiye.

[32] Türkiye Earthquake Hazard Maps Interactive Web Application TEHM (2021) Disaster and Emergency Management Presidency. Available at: https://tdth.afad.gov.tr/TDTH.

[33] Pacific Earthquake Engineering Research Center (PEER) (2014) PEER NGA Ground Motion Database. Available at: https://ngawest2.berkeley.edu/site.

[34] SeismoSoft (2018) SeismoMatch – A Computer Application Capable of Adjusting Earthquake Accelerograms to Match a Specific Target Response Spectrum.

[35] Chadwell CB, Imbsen RA (2004) XTRACT – A tool for axial force-ultimate curvature interactions. In: Structures 2004: Building on the Past, Securing the Future.